MRS Communications (2019), *9*, 1311–1316
© The Author(s) 2019
doi:10.1557/mrc.2019.127

MRS Communications

Research Letter

Anisotropic thermal conductivity in direction-specific black phosphorus nanoflakes

Heguang Liu, School of Materials Science and Engineering, Xi'an University of Technology, Xi'an 710048, China†
Jianxi Liu, State Key Laboratory of Solidification Processing, Center of Advanced Lubrication and Seal Materials, Northwestern Polytechnical University, Xi'an 710072, China†
Ruixuan Jing, and **Caiyin You,** School of Materials Science and Engineering, Xi'an University of Technology, Xi'an 710048, China
Address all correspondence to Heguang Liu at **heguangliu@xaut.edu.cn**

(Received 3 July 2019; accepted 5 September 2019)

Abstract

Herein, the authors report our pioneering demonstration of the anisotropic thermal properties of black phosphorus (BP) nanoflakes. The nanoflakes were produced using a scotch tape-based mechanical exfoliation technique. Their thickness was characterized using Atomic Force Microscopy The anisotropic direction of the nanoflakes was determined by the Raman Spectroscopy equipped with a polarized laser. Then, a temperature-dependent Raman spectroscopy method was utilized to study the thermal transport properties of the BP nanoflakes. The results indicated that the thermal conductivities of zigzag BP and armchair nanoflakes are 30.6 and 12.6 W/m·K, respectively. This fundamental thermal study gives insight into the future fabrication of nanoscale electronic devices with thermal properties that can be well controlled.

Introduction

Two-dimensional (2D)-layered nanomaterials, such as graphene and molybdenum disulfide (MoS_2), have become increasingly popular because of their outstanding electrical, optical, and mechanical properties.[1–3] The discovery and success of these materials have inspired black phosphorus (BP) to be viewed recently as a new nanomaterial in the 2D family. Unlike graphene with zero band gap[4] and MoS_2 which has a band gap of ~1.8 eV as a monolayer,[5] BP has been shown to have a thickness-dependent direct band gap varying from ~0.3 eV in its bulk form to greater than 1.5 eV as a monolayer.[6] The structure of BP is highly asymmetric and provides unusually strong in-plane anisotropy in orthogonal directions along what are called the Zigzag (ZZ) and Armchair (AC) directions.[7–9] Moving along the two different lattice directions renders different properties to be exhibited based on the phonon–phonon interactions among other attributes. Although it shows promise as a semiconductor material, its elementary electrical and thermal conductivities have yet to be fully characterized and documented.

Monolayer and few-layer BP nanoflakes can be produced by a traditional Scotch tape-based mechanical exfoliation technique often used in obtaining graphene from graphite.[10] The repeated "peeling" of bulk BP using scotch tape causes the puckered layers of BP to come apart. Compared to graphene, the van der Waals forces are greater between the BP layers and make it difficult to obtain a monolayer, but few-layer and multi-layer BP are readily available using this technique. Raman spectroscopy is used to identify and characterize materials.[5,11] BP has three characteristic Raman vibrational modes: A_g^1 (out of plane), B_{2g} (ZZ), and A_g^2 (AC).[12] Since vibrational information is specific to chemical bonds and the symmetry of molecules, a basic fingerprint is provided by which the materials can be ascertained.[13–16] Raman spectroscopy can also be used to determine lattice directions.[17,18] Since BP is highly anisotropic, polarized Raman measurements will cause the Raman peak in the direction chosen to be more intense.[19] Therefore, when the polarized laser is aligned along the ZZ direction, the B_{2g} vibrational mode will be more intense and the same is true along the AC direction. Polarized Raman spectroscopy provides a simple but effective way to determine the lattice directions of BP flakes. Preliminary thermal and electrical property measurements have been completed on few-layer BP flakes.[20]

For the electrical properties of BP materials, theoretical simulations have stated that electron and hole mobilities are significantly higher along the AC direction by a factor of about 2. The conductivity in the AC direction was reported as 14.58 μS and about 7.54 μS in the ZZ direction.[21] However, the anisotropic thermal properties of BP nanoflakes have not been well studied so far. Herein, the fabricated BP nanoflakes were measured for their thermal conductivity based on steady-state longitudinal heat flow using suspended-pad micro-devices. The

† These authors contributed equally to this work.

https://doi.org/10.1557/mrc.2019.127 Published online by Cambridge University Press

measurements were conducted on relatively thick (10–100 nm) nanoflakes over a wide temperature range (20–100 °C). The results provide a fundamental understanding of the thermal properties on BP nanoflakes according to their anisotropic structure. As opposed to isotropy, the anisotropy of BP causes the material's properties to be directionally dependent. This basic understanding will give insight into the future fabrication of nanoscale electronic devices with thermal properties that can be well controlled.

Experimental details

The BP nanoflakes were obtained by a typical Scotch tape-based mechanical exfoliation method.[10] Briefly, a silicon substrate with numerous 10 μm-wide trenches was first cleaned with a 20% HF solution for 1 min to remove the surface oxide layer. The substrate was immediately switched into a nitrogen-based glove box. The bulk BP flakes adhered on the Scotch tape were uniformly settled on the substrate and gently pressed for several times. The sample was put in the glove box for 5 min and then the Scotch tape was removed slightly. Such exfoliation process was repeated for three to five times on the same substrate to obtain the final BP nanoflake-attached sample for the thermal conductivity measurement.

The temperature-dependent Raman spectroscopic system was used to determine the thermal conductivity of various BP nanoflakes. The thermal conductivity calculation is based on the linear dependence of their phonon frequency on the sample temperature.[22,23] An external heating stage was used to vary the sample temperature to obtain the temperature coefficient. As mentioned above, the BP nanoflakes were suspended across two sides of the trenches in the silicon substrate that acted as the heat sink. The measurements were carried out using the HORIBA LabRAM confocal micro-Raman spectroscopy, which allows us to restrict the BP sampling volume to the suspended portion of the nanoflakes. A Raman laser with a wavelength of 532 nm and a spot size of 2 μm was focused at the center of the suspended BP nanoflakes. The spectra resolution of our Raman system is 0.1 cm^{-1}. Unlike the measurement for 2D graphene and MoS_2 materials,[24] the calculation in the current study is based on the one-dimensional heat conduction along directional BP nanoflakes.[19,25] When the optical laser heating was applied at the center of the nanoflakes, the heat transfer across the trench direction can be expressed by the basic Fourier's Law:

$$\frac{\partial Q}{\partial t} = K \oint \nabla T \cdot dA, \tag{1}$$

where K is the thermal conductivity, Q is the amount of heat transferred over the time t, T is the absolute temperature, and A is the cross-section area of BP nanoflakes expressed by $A = h \times W$ (h and W represent the thickness and width of BP nanoflakes, respectively). Equation (1) can be further written as:

$$\frac{\partial Q}{\partial t} = -K \cdot A \cdot \frac{\partial T}{\partial x}, \tag{2}$$

In the long heat conduction path,

$$\frac{\Delta Q}{\Delta t} = -K \cdot A \cdot \frac{\Delta T}{\Delta x}, \tag{3}$$

$$P = -K \cdot Wh \cdot \frac{T - T_0}{L/2}, \tag{4}$$

The change of laser power P leads to the variation of sample temperature T, thus,

$$P_2 - P_1 = -K \cdot Wh \cdot \frac{T_2 - T_1}{L/2}. \tag{5}$$

Considering the linear relationship between the Raman mode frequency and laser power or sample temperature, Eq. (5) can be derived as the following:

$$K = \frac{L}{2hW} \cdot \frac{\Delta P}{\Delta T} = \frac{L}{2hW} \cdot \frac{\Delta P}{\Delta T} = \frac{L}{2hW} \cdot \frac{\Delta\omega/\Delta T}{\Delta\omega/\Delta P} = \frac{L}{2hW} \cdot \frac{\chi_T}{\chi_P}. \tag{6}$$

Thus, we get,

$$K = \frac{L}{2hW} \cdot \frac{\chi_T}{\chi_P}, \tag{7}$$

where L is the length of BP nanoflakes suspended across the silicon channel, χ_T is the first-order temperature coefficient expressed as $\omega(T) = \omega_0 + \chi_T \cdot T$, and $\omega(P) = \omega_0' + \chi_P \cdot P$ is the change of phonon frequency with incident laser power. χ_T was obtained by measuring the phonon frequency at different temperatures, which was controlled by the Linkam DSC600 heating stage equipped with a T95-LINK PC interface controller. χ_T was obtained by measuring the phonon frequency at different laser power from 0 to 120 μW. The actual laser power absorbed by BP nanoflakes was estimated by $P = P_0 - P_1 = \tau \cdot P_0$, where P_0 is the incident laser power and P_1 is the laser power that transmitted the nanoflake.

Results and discussion

The goal of this study is to determine the relationship between the thermal properties of BP nanoflakes with the ZZ and AC directions. The atomic structure of the BP nanoflakes is shown in Fig. 1(a). Beginning with bulk BP, the nanoflakes were peeled off using the Scotch tape method made popular with graphene.[11] This mechanical exfoliation method allowed BP flakes around 10–100 nm in thickness to be developed. This method also allowed for preferable large flakes (>20 μm in length and width) to be produced. Due to the puckered atomic structure of BP, the van der Waals attractions between the phosphorus atoms are stronger than the flat nature of the carbon atoms in graphene, causing thinner films to be more difficult to obtain. Although research is currently being done to find other methods of producing BP thin films, the mechanical

https://doi.org/10.1557/mrc.2019.127 Published online by Cambridge University Press

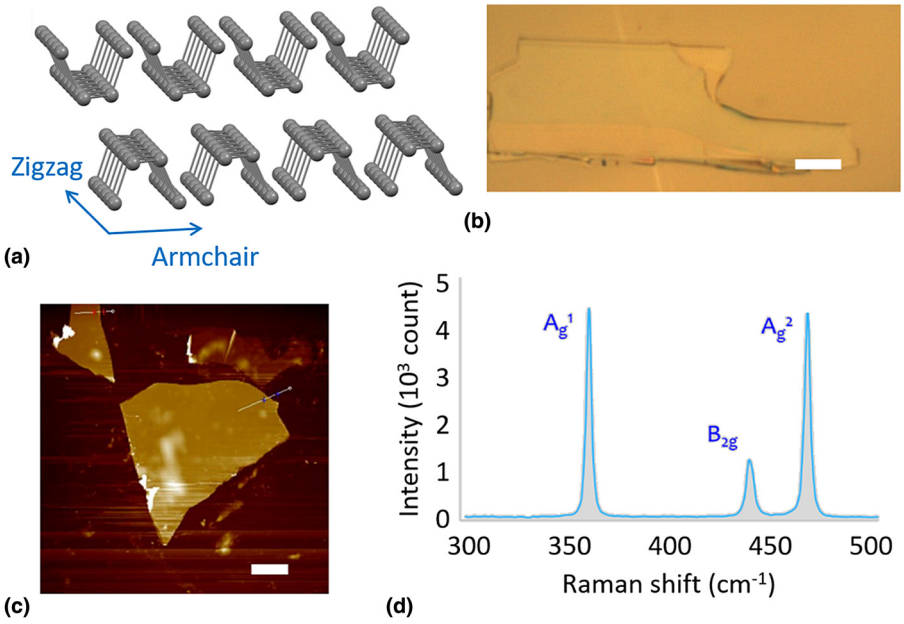


Figure 1. Exfoliation of BP nanoflakes. (a) Atomic structure of BP. (b) Optical image of an exfoliated BP nanoflake. (c) AFM image of the BP nanoflakes. (d) Raman characteristics of the BP nanoflakes. Scale bar: 5 μm.

exfoliation method is still a cheap and reliable way to obtain the necessary flakes.

Once flakes of BP obtained from mechanical exfoliation are shown in Fig. 1(b), the thicknesses were measured by the Atomic Force Microscopy (AFM) for calculating the thermal conductivity. The nanoflakes chosen for AFM measurements were first characterized under an optical microscope to make sure the flakes were large enough (>20 μm) in length and width [Fig. 1(c)]. The thickness of the nanoflakes (10–100 nm) was used as an important parameter for the thermal conductivity calculations as indicated in Eq. (7). It is worth noting that since BP is also unstable in ambient conditions, bubbles can form when surface oxidation occurs. When this happens, AFM will show that these bubbles are much higher than the actual flake's thickness, causing white dots to be visible in the AFM images. This provides a good way to estimate when a sample is no longer usable for testing the thermal and electrical properties. A typical Raman spectrum of the obtained BP nanoflakes is shown in Fig. 1(d). Similar to that mentioned above, the nanoflakes show three characteristic Raman vibrational modes: A_g^1, B_{2g}, and A_g^2, assigned to their different structural directions including out of plane, ZZ direction, and AC direction.[12–16]

Thermal conductivity values were obtained using a simple, reliable, and accurate Raman Spectroscopy technique.[22–24] The set-up is schematically shown in Fig. 2(a). Nanoflakes of BP were suspended across a trench of silicon and the Raman laser was turned on at the center of the flake. A 532 nm neon laser with a spot size of 2 μm was used as the optical heating source. The laser heats the BP flake and this heat travels towards the side [Fig. 2(b)]. SEM images of the silicon trench without and with the BP nanoflakes are shown in Figs. 2(c) and 2(d). The thermal conductivity measurement mainly includes the following steps: (1) Estimate the structural direction of the BP nanoflakes using a polarized Raman spectroscopy. (2) Measure the relationship between the peak position of Raman models and the sample temperature [temperature coefficient, $\omega(T)$]. To change the substrate temperature, the substrate was kept in a chamber with a heating bed during the measurements. This chamber also served as a way to prevent surface oxidation by pumping out oxygen air and replacing the air with nitrogen gas. (3) Measure the relationship between the peak position of Raman models and the laser power [power coefficient, $\omega(P)$]. (4) When the two coefficients are found, they are plugged into Eq. (7) to obtain the thermal conductivity values.

As we mentioned above, before conducting the thermal conductivity measurement, it is essential to define the direction (AC or ZZ) of the obtained BP nanoflakes. Once large flakes of BP were found, polarized Raman spectroscopy was performed to determine the two directions on the chosen flake.[26–28] The Raman laser was initially polarized to a specific direction for all the BP samples. As the laser was polarized and becomes aligned with one of the two lattice directions, the corresponding vibrational peak will become more intense. Based on the intensity of the vibrational modes, the ZZ and AC directions can be determined and nanoflake can be fabricated orthogonally on the flake. As shown in Fig. 3, two nanoflakes in the AC direction and ZZ direction were selected, respectively [Figs. 3(a) and 3(d)]. These directions were determined at 90 °C polarization. This degree mark was chosen

https://doi.org/10.1557/mrc.2019.127 Published online by Cambridge University Press

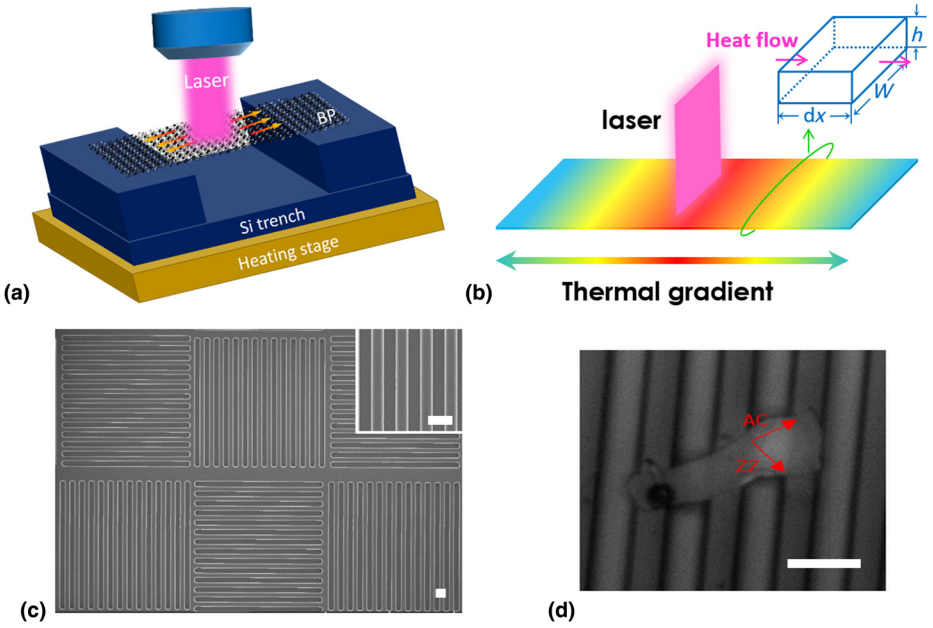


Figure 2. Raman set-up for the thermal measurement. (a) Schematic of the set-up. (b) Laser-induced thermal transfer in a BP nanoflake. (c) Silicon trenches fabricated by the photolithographic method. (d) A BP nanoflake suspended on the trench. Scale bar: 10 μm.

because when the laser is polarized at 90 °C, the laser is in line with the lattice direction running across the trenches [Figs. 3(b) and 3(e)]. When the intensity of the A_g^2 Raman peak is highest at 90 °C, the direction across the trench is understood to be in the AC direction [Figs. 3(c) and 3(f)]. As shown in Fig. 3(c), when the B_{2g} intensity is highest, the direction tested will be in the ZZ direction. These three flakes allow for contrasting results to be observed when testing thermal conductivity. This is important for understanding which direction has better thermal properties.

As depicted in Fig. 4(a), the temperature was increased from room temperature to 100 °C using a heating stage underneath the silicon substrate. As the temperature increased, we observed an obvious redshift of the Raman spectra. In Fig. 4(b), the laser power was increased from 0.218 to 103 μW which correspond to 0.01% and 5% of the total laser power, respectively. As the

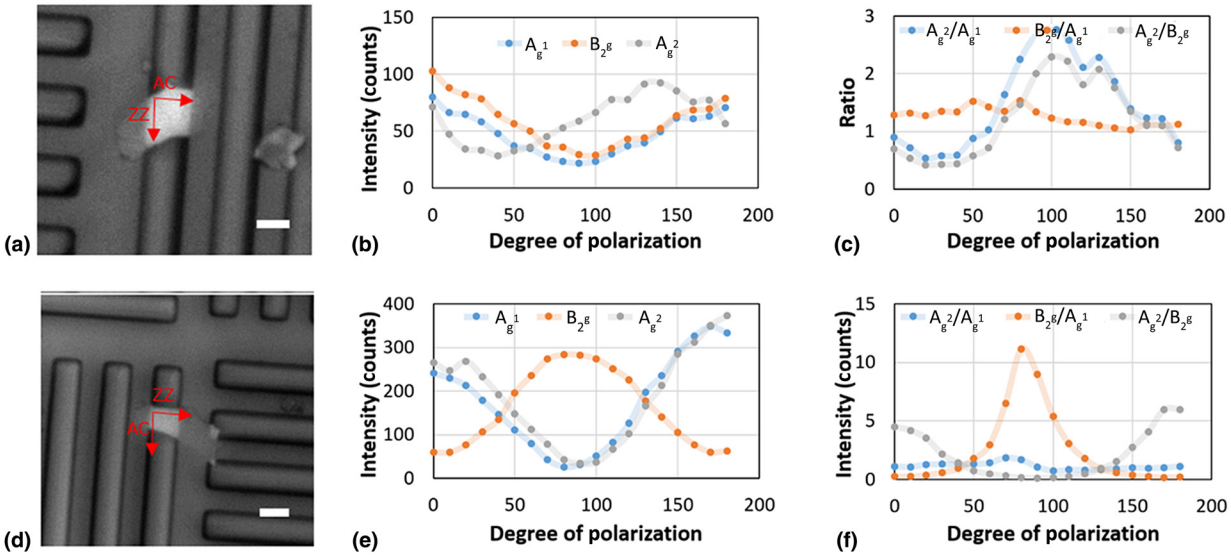


Figure 3. Raman polarization measurement. (a) A suspended AC BP nanoflake, (b) its Raman peak intensity, and (c) the Raman peak ratio. (d) A suspended ZZ BP nanoflake, (e) its Raman peak intensity, and (f) the Raman peak ratio. Scale bar: 5 μm.

https://doi.org/10.1557/mrc.2019.127 Published online by Cambridge University Press

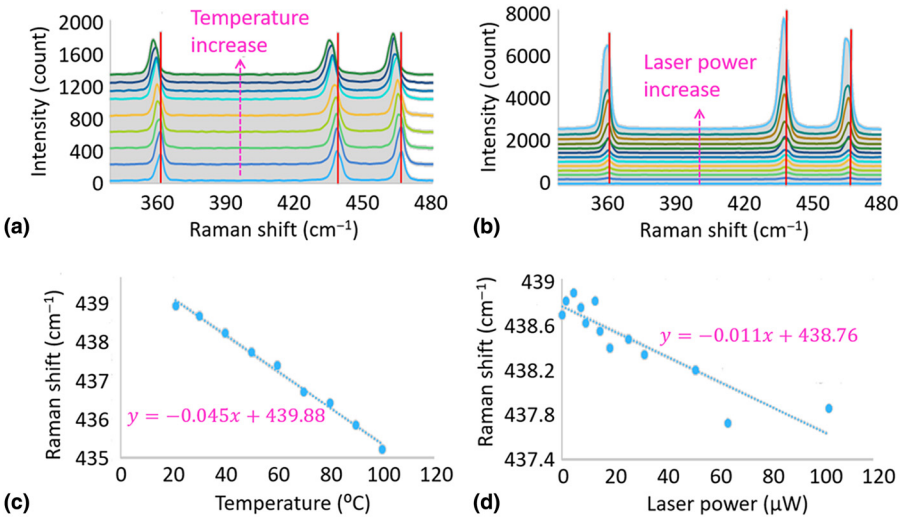


Figure 4. Thermal conductivity measurement. (a) Raman spectra at various temperatures. (b) Raman spectra at various laser power. (c) B_{2g} peak location as a function of the temperature. (d) B_{2g} peak location as a function of the laser power.

laser power increased, the Raman spectra are also red-shifted. The Raman shift positions were collected and plotted in a linear trend where the slopes are the temperature and power coefficients as shown in Figs. 4(c) and 4(d), respectively. Using the thermal conductivity equation mentioned earlier, the conductivity in the armchair direction for Flake 1 and zigzag direction for Flake 2. The thermal conductivities for the AC direction and the ZZ direction were 12.62 and 30.61 W/m·K, respectively. The Raman spectroscopy method used to measure and calculate the thermal conductivity was successful in obtaining accurate results. The values that were observed were similar to those discovered in recent literatures.[29–32] Based on the thermal conductivity results, the ZZ direction in the BP crystal lattice had a higher value than that of the AC direction. These values indicate that the ZZ direction is better than the AC direction at conducting heat. The results were found using a very simple and accurate Raman spectroscopy technique which will be easier to implement in future works. Since the instability of BP is always a large limitation of the material, also understanding the effect of surface oxidation on the thermal conductivity and electrical properties will be important for device applications.

Conclusions

To sum up, this work provides a fundamental understanding of the relationship of thermal conductivity of black phosphorous nanoflake in different structural direction. The thermal conductivity values of both the AC and ZZ directions were calculated using a facial Raman spectroscopy technique, yielding higher conductivity in the ZZ direction. The results indicate that BP nanoflakes will allow for better heat management in nanoscale electronics. This study provides a direct reference for the fabrication of BP-related electronic devices where the thermal transfer behaviors have to be considered.

Acknowledgments

This work was partly supported by National Natural Science Foundation of China (No. 51802258) and project funded by the China Postdoctoral Science Foundation (No. 2018M643698).

References

1. K.S. Novoselov, A.K. Geim, S.V. Morozov, D. Jiang, Y. Zhang, S.V. Dubonos, I.V. Grigorieva, and A.A. Firsov: Electric field effect in atomically thin carbon films. *Science* **306**, 666 (2004).
2. Y. Li and N. Chopra: Progress in large-scale production of graphene. Part 2: vapor methods. *JOM* **67**, 44 (2015).
3. A. Splendiani, L. Sun, Y. Zhang, T. Li, J. Kim, C.Y. Chim, G. Galli, and F. Wang: Emerging photoluminescence in monolayer MoS_2. *Nano Lett.* **10**, 1271 (2010).
4. F. Schedin, A.K. Geim, S.V. Morozov, E.W. Hill, P. Blake, M.I. Katsnelson, and K.S. Novoselov: Detection of individual gas molecules adsorbed on graphene. *Nat. Mater.* **6**, 652 (2007).
5. K.F. Mak, C. Lee, J. Hone, J. Shan, and T.F. Heinz: Atomically thin MoS_2: a new direct-gap semiconductor. *Phys. Rev. Lett* **105**, 136805 (2010).
6. A. Castellanos-Gomez, L. Vicarelli, E. Prada, J.O. Island, K.L. Narasimha-Acharya, S.I. Blanter, D. Groenendijk, M. Buscema, G.A. Steele, J.V. Alvarez, H.W. Zandbergen, J.J. Palacios, and S.J. Van der Zant: Isolation and characterization of few-layer black phosphorus. *2D Mater.* **1**, 025001 (2014).
7. F. Xia, H. Wang, and Y. Jia: Rediscovering black phosphorus as an anisotropic layered material for optoelectronics and electronics. *Nat. Commun.* **5**, 4458 (2014).
8. Q. Li, H. Huang, Z. Chen, X. Huang, K. Deng, S. Luo, and Z. Quan: Thickness-dependent structural stability and anisotropy of black phosphorus. *Adv. Electron. Mater.* **5**, 1800712 (2019).
9. Y. Liu, T. Low, and P.P. Ruden: Mobility anisotropy in monolayer black phosphorus due to scattering by charged impurities. *Phys. Rev. B* **93**, 165402 (2016).
10. A. Favron, E. Gaufrès, F. Fossard, P. Lévesque, A. Phaneuf-L'Heureux, N. Tang, and R. Martel: Exfoliating pristine black phosphorus down to the monolayer: photo-oxidation and electronic confinement effects. *arXiv Preprint* **1408**, 0345 (2014).
11. A.K. Geim and K.S. Novoselov: The rise of graphene. *Nat. Mater.* **6**, 183 (2007).

https://doi.org/10.1557/mrc.2019.127 Published online by Cambridge University Press

12. V. Tran, R. Soklaski, Y. Liang, and L. Yang: Layer-controlled band gap and anisotropic excitons in few-layer black phosphorus. *Phys. Rev. B* **89**, 235319 (2014).
13. Y. Li, W. Shi, and N. Chopra: Functionalization of multilayer carbon shell-encapsulated gold nanoparticles for surface-enhanced Raman scattering sensing and DNA immobilization. *Carbon* **100**, 165 (2016).
14. Y. Li, J. Dykes, T. Gilliam, and N. Chopra: A new heterostructured SERS substrate: free-standing silicon nanowires decorated with graphene-encapsulated gold nanoparticles. *Nanoscale* **9**, 5263 (2017).
15. J. Kang, J.D. Wood, S.A. Wells, J.-H. Lee, X. Liu, K.-S. Chen, and M.C. Hersam: Solvent exfoliation of electronic-grade, two-dimensional black phosphorus. *ACS Nano* **9**, 3596 (2015).
16. S. Liu, N. Huo, S. Gan, Y. Li, Z. Wei, B. Huang, and H. Chen: Thickness-dependent Raman spectra, transport properties and infrared photoresponse of few-layer black phosphorus. *J. Mater. Chem. C* **3**, 10974 (2015).
17. Y. Li, Z. Hu, S. Lin, S.K. Lai, W. Ji, and S.P. Lau: Giant anisotropic Raman response of encapsulated ultrathin black phosphorus by uniaxial strain. *Adv. Funct. Mater.* **27**, 1600986 (2017).
18. H. Liu, A.T. Neal, Z. Zhu, Z. Luo, X. Xu, D. Tománek, and P.D. Ye: Phosphorene: an unexplored 2D semiconductor with a high hole mobility. *ACS Nano* **8**, 4033 (2014).
19. Y. Li, E.C. Moy, A.A. Murthy, S. Hao, J.D. Cain, E.D. Hanson, and X. Chen: Large-scale fabrication of MoS_2 ribbons and their light-induced electronic/thermal properties: dichotomies in the structural and defect engineering. *Adv. Funct. Mater.* **28**, 1704863 (2018).
20. P. Chen, N. Li, X. Chen, W.J. Ong, and X. Zhao: The rising star of 2D black phosphorus beyond graphene: synthesis, properties and electronic applications. *2D Mater.* **5**, 014002 (2017).
21. J. Tao, W. Shen, S. Wu, L. Liu, Z. Feng, C. Wang, and W. Pang: Mechanical and electrical anisotropy of few-layer black phosphorus. *ACS Nano* **9**, 11362–11370 (2015).
22. A.A. Balandin, S. Ghosh, W. Bao, I. Calizo, D. Teweldebrhan, F. Miao, and C.N. Lau: Superior thermal conductivity of single-layer graphene. *Nano Lett.* **8**, 902 (2008).
23. Y. Li and N. Chopra: Chemically modified and doped carbon nanotube-based nanocomposites with tunable thermal conductivity gradient. *Carbon* **77**, 675 (2014).
24. R. Yan, J.R. Simpson, S. Bertolazzi, J. Brivio, M. Watson, X. Wu, and H.G. Xing: Thermal conductivity of monolayer molybdenum disulfide obtained from temperature-dependent Raman spectroscopy. *ACS Nano* **8**, 986 (2014).
25. A.A. Balandin: Thermal properties of graphene and nanostructured carbon materials. *Nat. Mater.* **10**, 569 (2011).
26. X. Wang, A.M. Jones, K.L. Seyler, V. Tran, Y. Jia, H. Zhao, and F. Xia: Highly anisotropic and robust excitons in monolayer black phosphorus. *Nat. Nanotechnol.* **10**, 517 (2015).
27. N. Mao, S. Zhang, J. Wu, H. Tian, J. Wu, H. Xu, and J. Zhang: Investigation of black phosphorus as a nano-optical polarization element by polarized Raman spectroscopy. *Nano Res.* **11**, 3154 (2018).
28. W. Zhu, L. Liang, R.H. Roberts, J.F. Lin, and D. Akinwande: Anisotropic electron–phonon interactions in angle-resolved Raman study of strained black phosphorus. *ACS Nano* **12**, 12512 (2018).
29. S. Lee, F. Yang, J. Suh, S. Yang, Y. Lee, G. Li, and C. Ko: Anisotropic in-plane thermal conductivity of black phosphorus nanoribbons at temperatures higher than 100 K. *Nat. Commun.* **6**, 8573 (2015).
30. Z. Luo, J. Maassen, Y. Deng, Y. Du, R.P. Garrelts, M.S. Lundstrom, and X. Xu: Anisotropic in-plane thermal conductivity observed in few-layer black phosphorus. *Nat. Commun.* **6**, 8572 (2015).
31. S.G. Jeon, H. Shin, Y.H. Jaung, J. Ahn, and J.Y. Song: Thickness-dependent and anisotropic thermal conductivity of black phosphorus nanosheets. *Nanoscale* **10**, 5985 (2018).
32. A. Islam, A. van den Akker, and P.X.L. Feng: Anisotropic thermal conductivity of suspended black phosphorus probed by opto-thermomechanical resonance spectromicroscopy. *Nano Lett.* **18**, 7683 (2018).

https://doi.org/10.1557/mrc.2019.127 Published online by Cambridge University Press